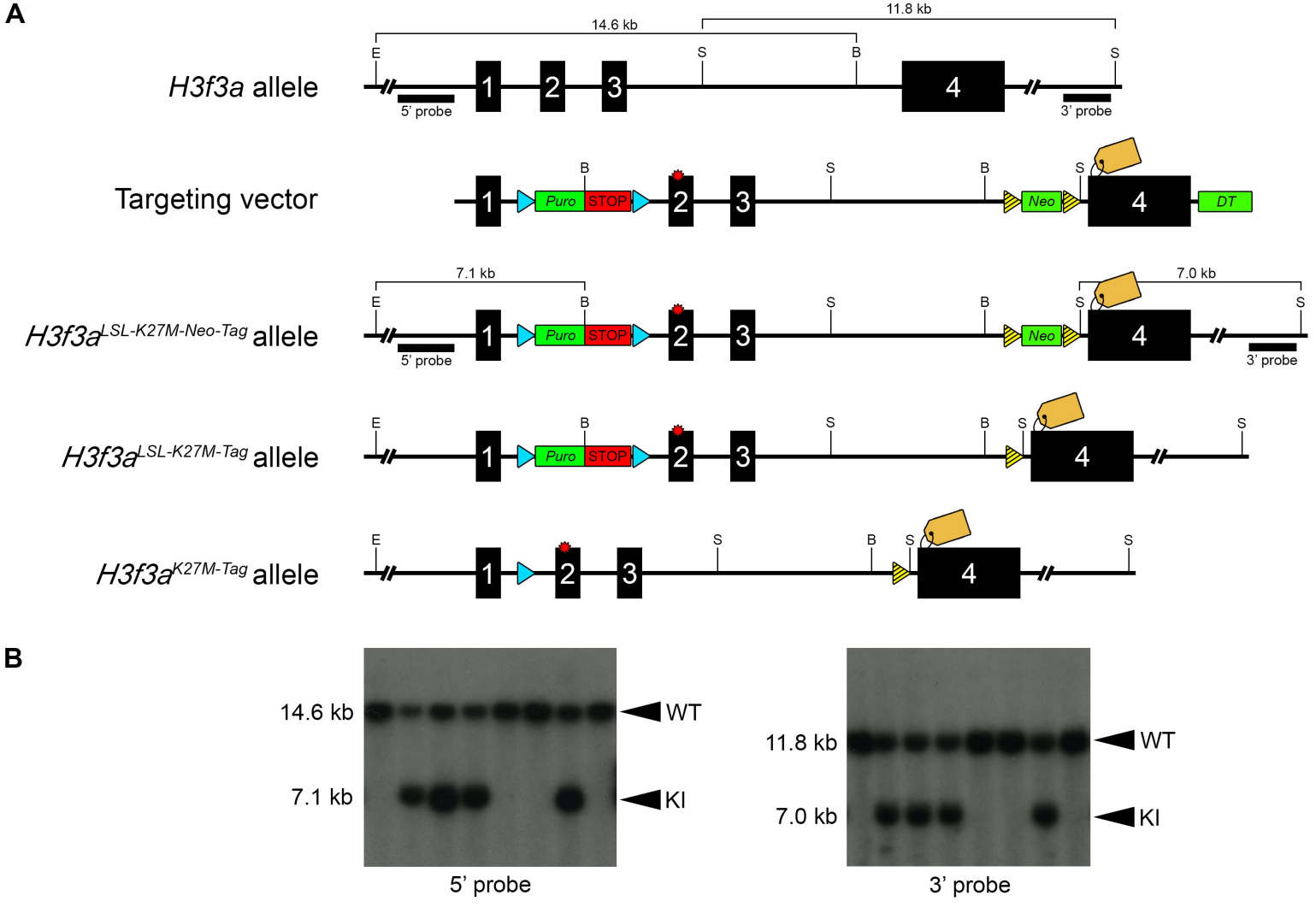
A
14.6 kb
11.8 kb
E
S
B
S
H3f3a allele
1
2
3
4
5' probe
3' probe
Targeting vector
B
S
B
S
Puro
STOP
Neo
DT
H3f3aLSL-K27M-Neo-Tag allele
7.1 kb
7.0 kb
H3f3aLSL-K27M-Tag allele
H3f3aK27M-Tag allele
B
14.6 kb
7.1 kb
WT
KI
5' probe
11.8 kb
7.0 kb
WT
KI
3' probe

Figure S1 (related to Figure 1). Design of Epitope-Tagged Conditional *H3f3a*$^{LSL\text{-}K27M\text{-}Tag}$ Knock-In Allele.

(A) Schematic of endogenous *H3f3a* allele, targeting vector, targeted allele before and after Flippase-mediated excision of the *Neo* cassette, and Cre-mediated excision of STOP cassette. *H3f3a* allele: Exons are indicated as numbered boxes. Restriction sites are indicated: E, *Eco*RI; S, *Sac*I; B, *Bam*HI. External 5' probe detects an endogenous 14.6 kb *Eco*RI/*Bam*HI-digested genomic DNA fragment. External 3' probe detects an endogenous 11.8 kb *Sac*I-digested genomic DNA fragment. Targeting Vector: STOP cassette equipped with Puromycin resistance (*Puro*) and STOP sequences flanked by *loxP* sites (turquois arrowheads) positioned in intron 1. Red star indicates K27M point mutation on exon 2. Neomycin resistance cassette (*Neo*) flanked by *Frt* sites (striped yellow arrowheads) positioned in intron 3. Epitope tag positioned in exon 4 (tan tag). Vector backbone Diphtheria toxin negative selection cassette (*DT*) positioned downstream of *H3f3a* exon 4. *H3f3a*$^{LSL\text{-}K27M\text{-}Neo\text{-}Tag}$ allele: Correctly targeted allele detected by 5' external probe hybridizing to 7.1 kb *Eco*RI/*Bam*HI-digested genomic DNA fragment, and a 3' external probe hybridizing to 7.0 kb *Sac*I-digested genomic DNA fragment. *H3f3a*$^{LSL\text{-}K27M\text{-}Tag}$ allele: Successful Flippase-mediated excision of the *Neo* cassette. *H3f3a*$^{K27M\text{-}Tag}$ allele: Knock-in allele after Cre-mediated excision of the STOP cassette. (B) Representative Southern blot screening of DNA from ES cell clones. Here, four clones with correctly targeted *H3f3a* allele were identified by both 5’ (left) or 3’ (right) probes.

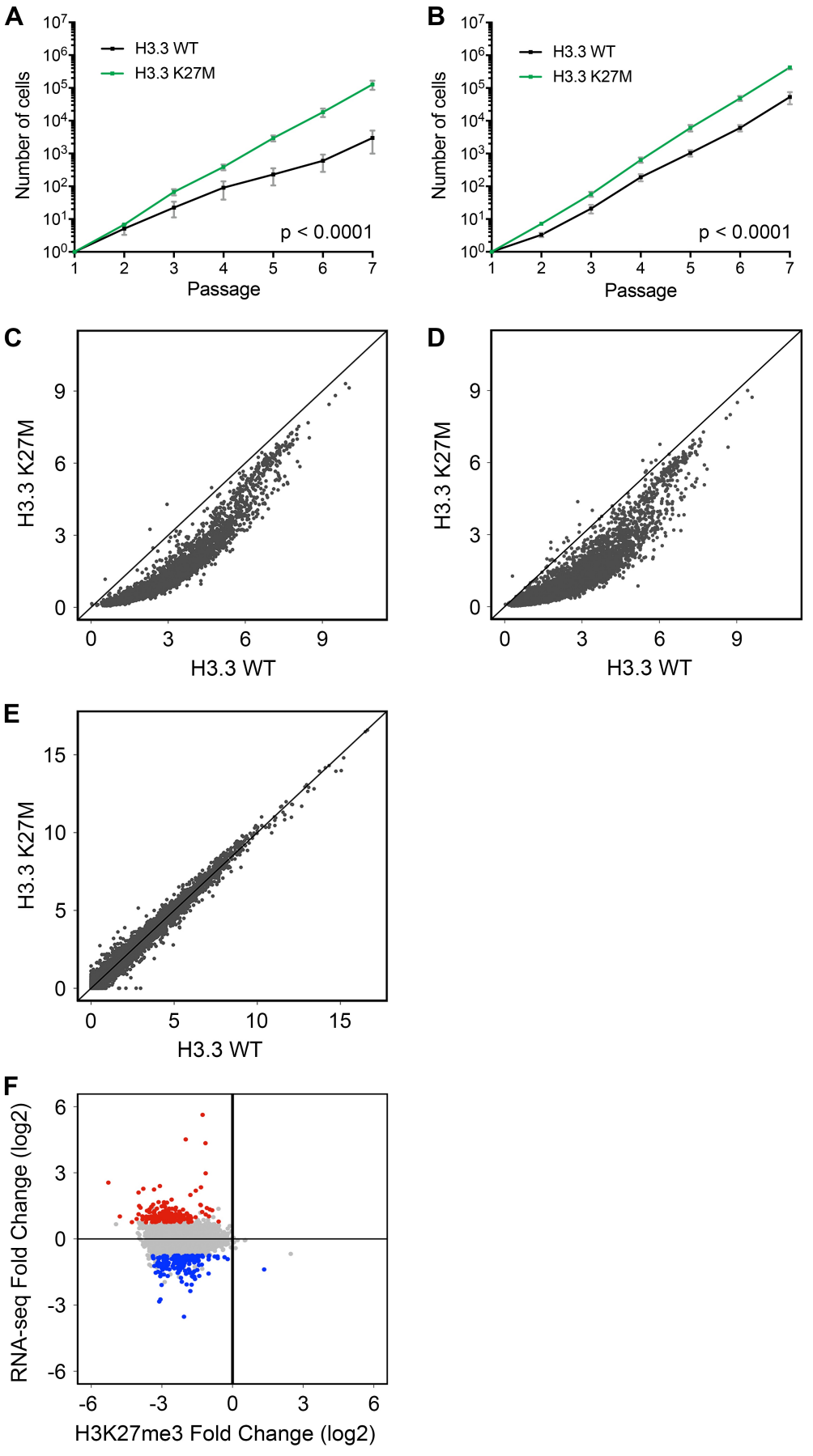
A
B
C
D
E
F
H3.3 WT
H3.3 K27M
Number of cells
Passage
p < 0.0001
H3.3 K27M
H3.3 WT
RNA-seq Fold Change (log2)
H3K27me3 Fold Change (log2)

Figure S2 (related to Figure 1). Region-Specific Signatures Maintained Despite H3.3 K27M Effects.

NSCs were isolated from forebrain and hindbrain (F- and H-NSC) of E15.5 embryos and grown as neurospheres. (A, B) Growth of F- (A) or H- (B) NSCs expressing H3.3 K27M (n = 4) or H3.3 WT (n = 2) were assayed over sequential passages by calculating mean cumulative cell numbers +/- SEM. $p < 0.0001$ for both (A) and (B). (C,D) Scatterplot comparing H3K27me3 ChIP-seq peak signal intensity (log2(CPM+1)) in H3.3 K27M versus H3.3 WT F- (C) and H- (D) NSCs. n = 3 in each genotype group for each region. (E) Scatterplot comparing expression levels in H3.3 K27M and H3.3 WT F-NSCs (RNA-seq plotted as log2(FPKM+1)). n = 3 in each group. (F) RNA-seq versus H3K27me3 in F-NSCs. Colored data points depict genes upregulated (red) and downregulated (blue) in H3.3 K27M, with $p < 0.05$ and a log2 fold change greater than 0.75 or less than -0.75, respectively, compared to the gene loci bulk (gray). n = 3 in each group. For all NSC experiments, n represents NSC cultures isolated from independent embryos.

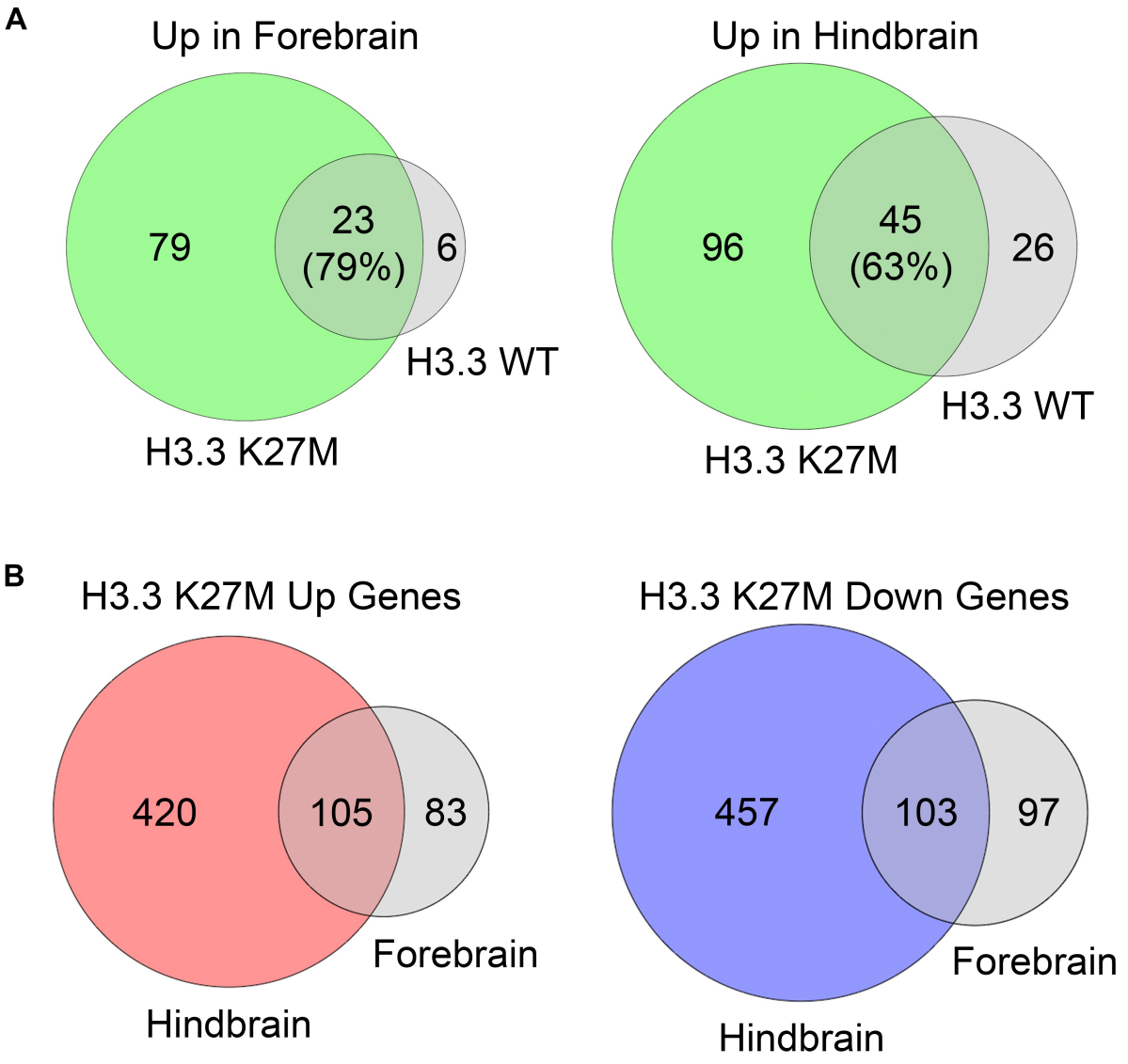

Figure S3 (related to Figure 1). Regional Gene Signatures and H3.3 K27M-Mediated Gene Expression Changes in Hindbrain and Forebrain NSCs.

(A) Venn diagrams showing the overlap of regional up-regulated gene signatures (defined as at least log2 two-fold expression increase, $p < 0.05$) in forebrain (versus hindbrain) or hindbrain (versus forebrain) within each genotype (H3.3 WT or H3.3 K27M). Intersection shows the number and percentage of forebrain or hindbrain genes regionally regulated in H3.3 WT that are also regionally regulated in H3.3 K27M NSCs. (B) Venn diagrams showing the overlap between the genes up-regulated and down-regulated by H3.3 K27M versus H3.3 WT (log2 fold change greater than 0.75 or less than -0.75, $p < 0.05$), respectively in either forebrain or hindbrain NSCs. Intersection shows shared genes upregulated by H3.3 K27M or downregulated by H3.3 K27M in both hindbrain and forebrain. (A,B) Number of genes in each area of the Venn diagrams is shown.

A

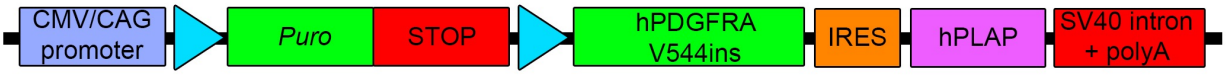

B

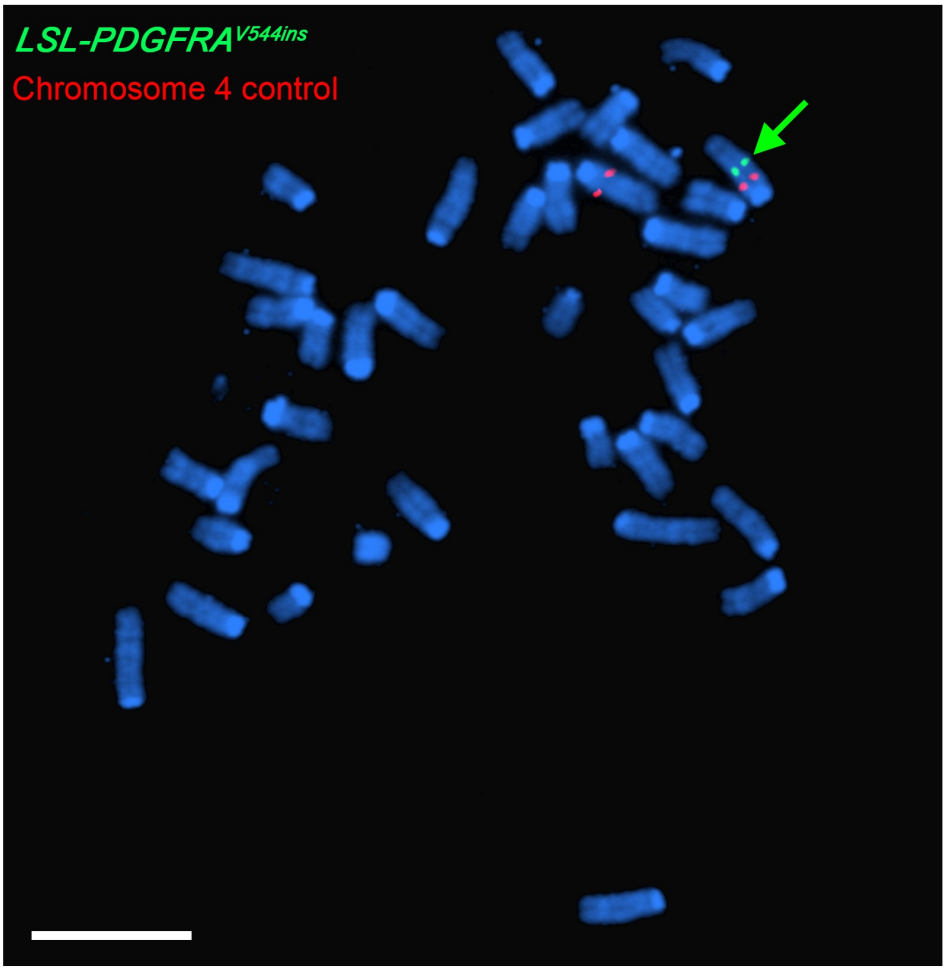

Figure S4 (related to Figure 3). Design of Conditional *LSL-PDGFRA*^{V544ins} Transgenic Allele.

(A) Schematic of conditional *PDGFRA*^{V544ins} transgene construct, containing a CMV/CAG promoter, STOP cassette equipped with Puromycin resistance (*Puro*) and STOP sequences flanked by *loxP* sites (turquois arrowheads), cDNA of mutant human *PDGFRA* (hPDGFRA V544ins), internal ribosome entry site (IRES), human placental alkaline phosphatase reporter gene (hPLAP), and SV40 splicing and polyadenylation signal (SV40 intron+polyA). (B) Fluorescence in situ hybridization (FISH) for the transgene (green), or control chromosome 4 probe (red), showing a single transgene integration site on chromosome 4. Scale bar = 10 μm.

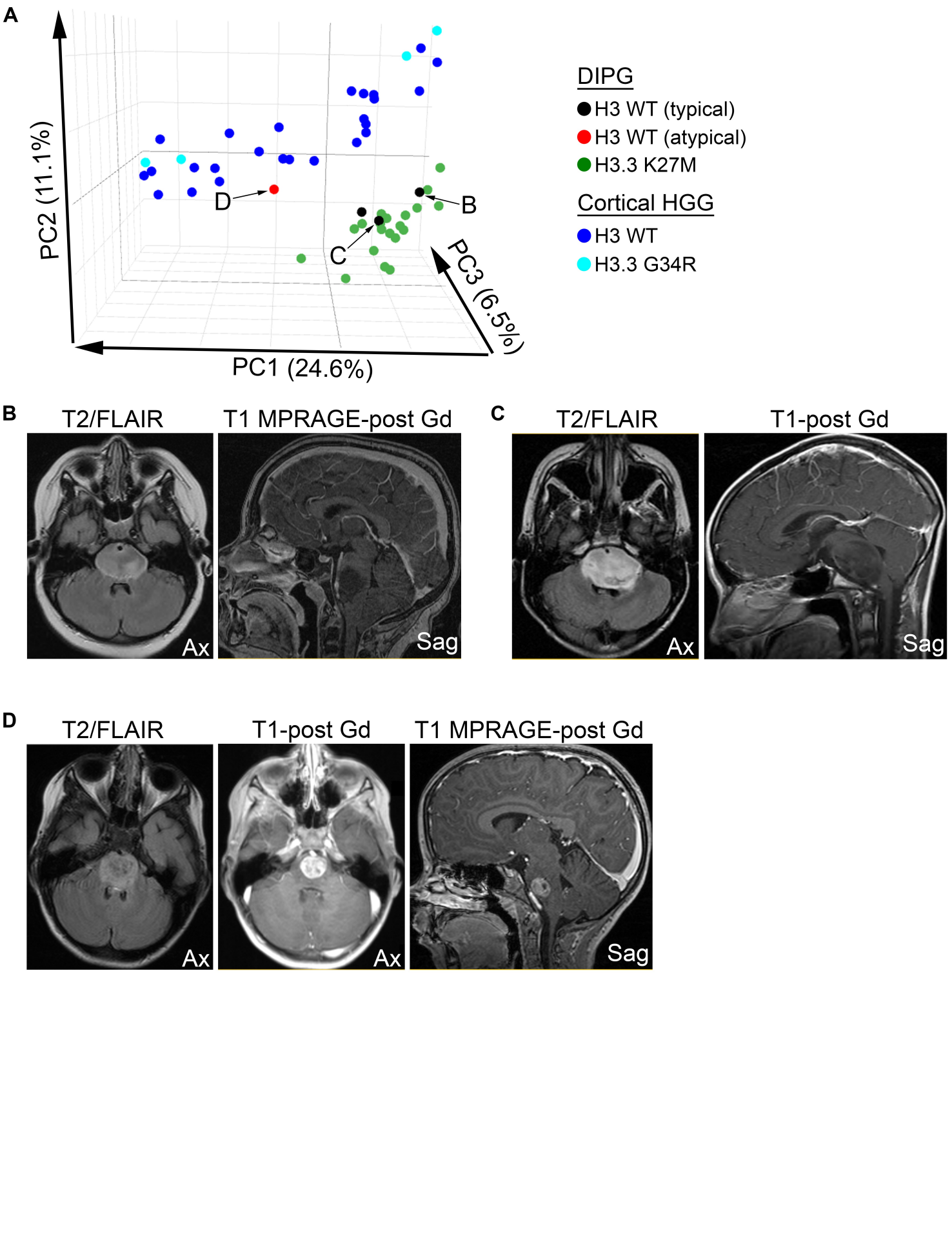
A
PC2 (11.1%)
PC1 (24.6%)
PC3 (6.5%)
D
C
B
DIPG
H3 WT (typical)
H3 WT (atypical)
H3.3 K27M
Cortical HGG
H3 WT
H3.3 G34R
B
T2/FLAIR
T1 MPRAGE-post Gd
Ax
Sag
C
T2/FLAIR
T1-post Gd
Ax
Sag
D
T2/FLAIR
T1-post Gd
T1 MPRAGE-post Gd
Ax
Ax
Sag

Figure S5 (related to Figure 5). Typical DIPGs Cluster Primarily By Brain Location, Not H3 Mutation Status.

(A) PCA (top 1000 most variable genes) of human HGGs including typical (n = 3) or atypical (n = 1) H3 WT DIPGs, H3.3 K27M DIPGs (n = 20), H3 WT cortical HGGs (n = 25) and H3.3 G34R cortical HGGs (n = 4). Percentage of variance captured by each component is reported on axes. Small arrows indicate tumors featured in panels below. (B-D) Magnetic Resonance Imaging (MRI) was available for three of the four H3 WT DIPGs. Axial view (Ax); Sagittal view (Sag). (B) Typical DIPG MRI: Axial T2-weighted fluid-attenuated inversion recovery (FLAIR) and sagittal postcontrast T1-weighted magnetization-prepared rapid gradient-echo (MPRAGE) images of the brain in a 5 year old patient. The tumor is non-enhancing and is centered on the ventral-inferior pons. In transverse images it involves about 85% of the cross-sectional area of the brainstem and engulfs the basilar artery ventrally but shows some sparing of the tegmentum dorsally. (C) Typical DIPG MRI: Axial postcontrast T2-weighted FLAIR and sagittal postcontrast T1-weighted images of the brain in an 8 year old patient. The minimally enhancing tumor involves almost the entire pons and extends to the upper medulla oblongata. Anterior exophytic growth results in engulfment of the basilar artery. These features are similar to those described in (B) and are considered typical for DIPG. (D) Atypical DIPG MRI: Axial postcontrast T2-weighted FLAIR, T1-weighted postcontrast and sagittal postcontrast T1-weighted MPRAGE images of the brain in a 6 year old patient. The location of the lesion would be characteristic of DIPG and the T2 signal abnormalities also involve almost the entire cross-sectional area of the brainstem. There is however a very well-defined, avidly enhancing central component suggesting a focal tumor and the surrounding, non-enhancing T2 signal changes could correspond to perilesional edema only. There is no engulfment of the basilar artery. Although some degree of enhancement within the tumor lesion is seen in up to 60-70% of patients with DIPG, it is usually less prominent, less well-defined and sometimes multifocal. Atypical DIPG shown in D was not included in molecular analyses with H3 WT DIPGs in this study.

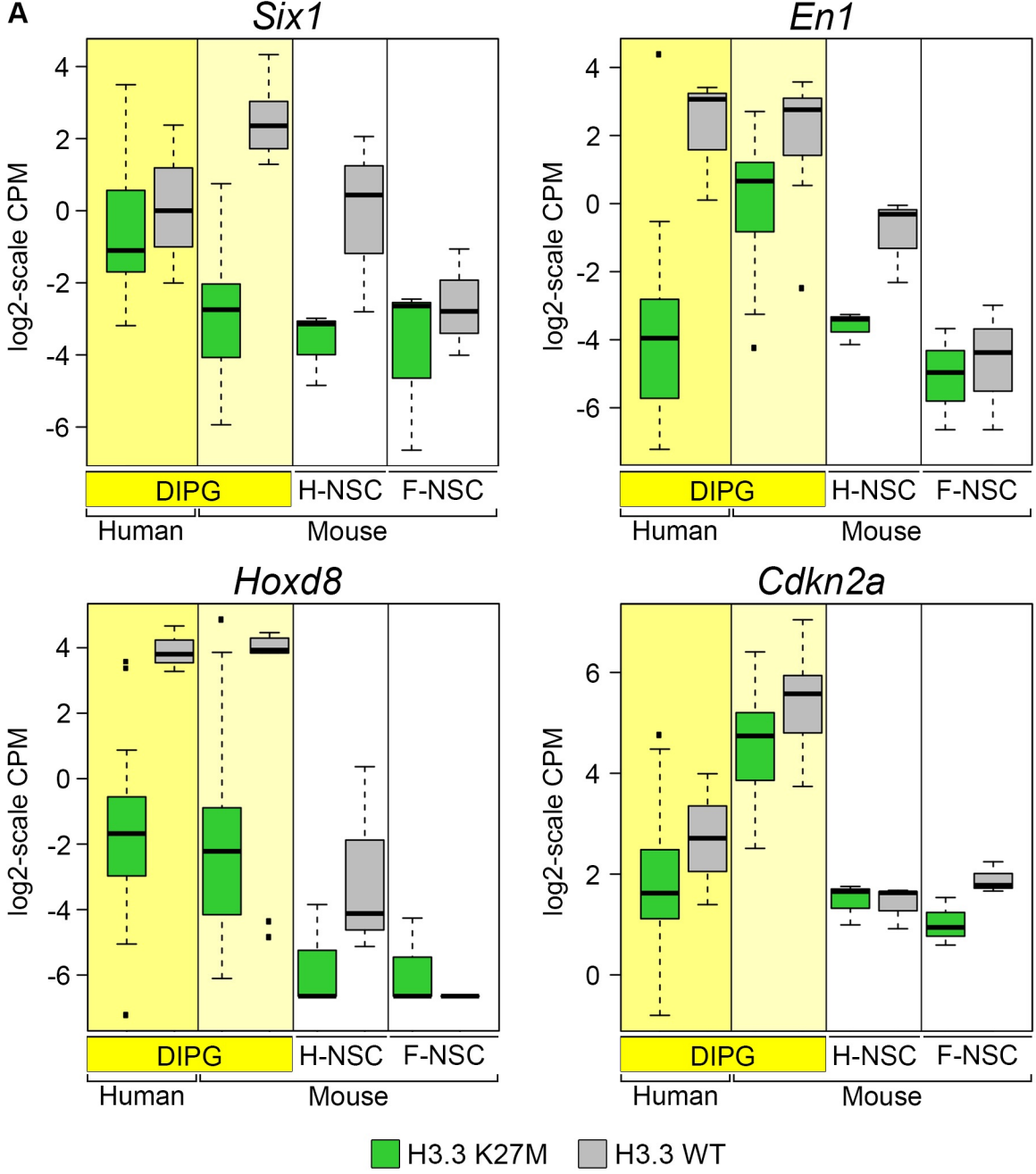
A
Six1
En1
Hoxd8
Cdkn2a
log2-scale CPM
DIPG
H-NSC
F-NSC
Human
Mouse
H3.3 K27M
H3.3 WT

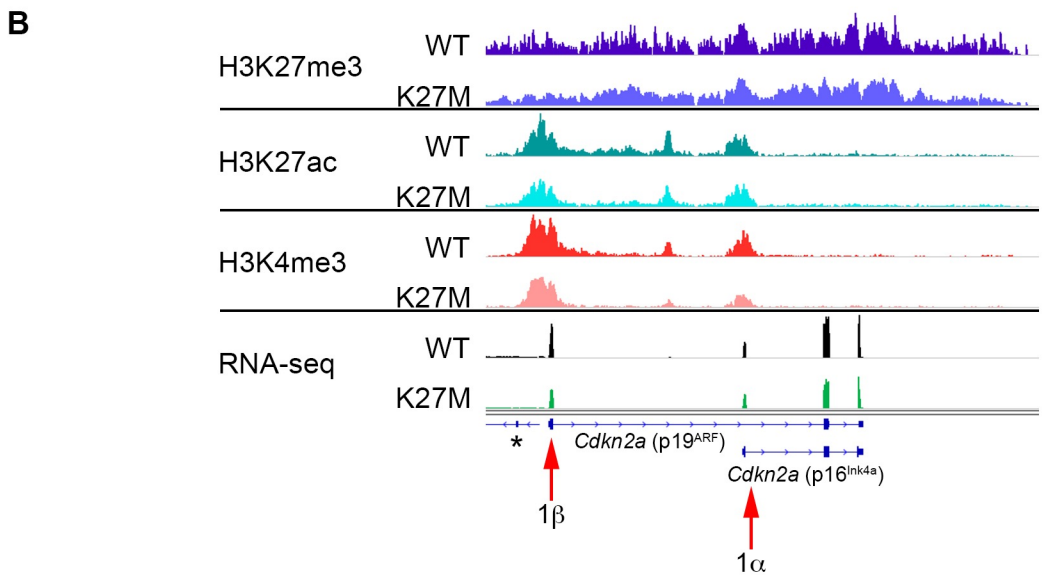
B
H3K27me3
H3K27ac
H3K4me3
RNA-seq
WT
K27M
Cdkn2a (p19ARF)
Cdkn2a (p16Ink4a)
1β
1α

Figure S6 (related to Figure 5). H3.3 K27M Downregulated Genes in Mouse DIPGs Show Similar Regulation in Human DIPGs.

(A) Expression of H3.3 K27M-dependent down-regulated genes *Six1*, *En1*, *Hoxd8*, and *Cdkn2a*. Boxplots depict log2-scale RNA-seq CPM values for primary human and mouse DIPGs, and mouse hindbrain (H-NSC) and forebrain (F-NSC) NSCs expressing H3.3 K27M or H3.3 WT. Box plots show the interquartile range (IQR). Median is shown as a horizontal line, highest and lowest values up to 1.5 times the IQR are shown with dotted lines outside box, and outliers greater than 1.5 times the IQR are shown as black squares. (B) Average tracks for *Cdkn2a* locus showing H3K27me3, H3K27ac and H3K4me3 enrichment and RNA-seq in H3.3 WT or H3.3 K27M expressing mouse DIPGs (identical scale for each genotype pair). * indicates *Gm12610* locus upstream of *Cdkn2a*. n = 6 (H3.3 K27M) and n = 5 (H3.3 WT) for H3K27me3 and H3K27ac; n = 2 (H3.3 K27M) and n = 3 (H3.3 WT) for H3K4me3; n = 20 (H3.3 K27M) and n = 9 (H3.3 WT) for RNA-seq. *Cdkn2a* encodes two tumor suppressor genes through expression of different first exons. Locations of exons 1α ($p16^{Ink4a}$) and 1β ($p19^{Arf}$) are marked with red arrows.

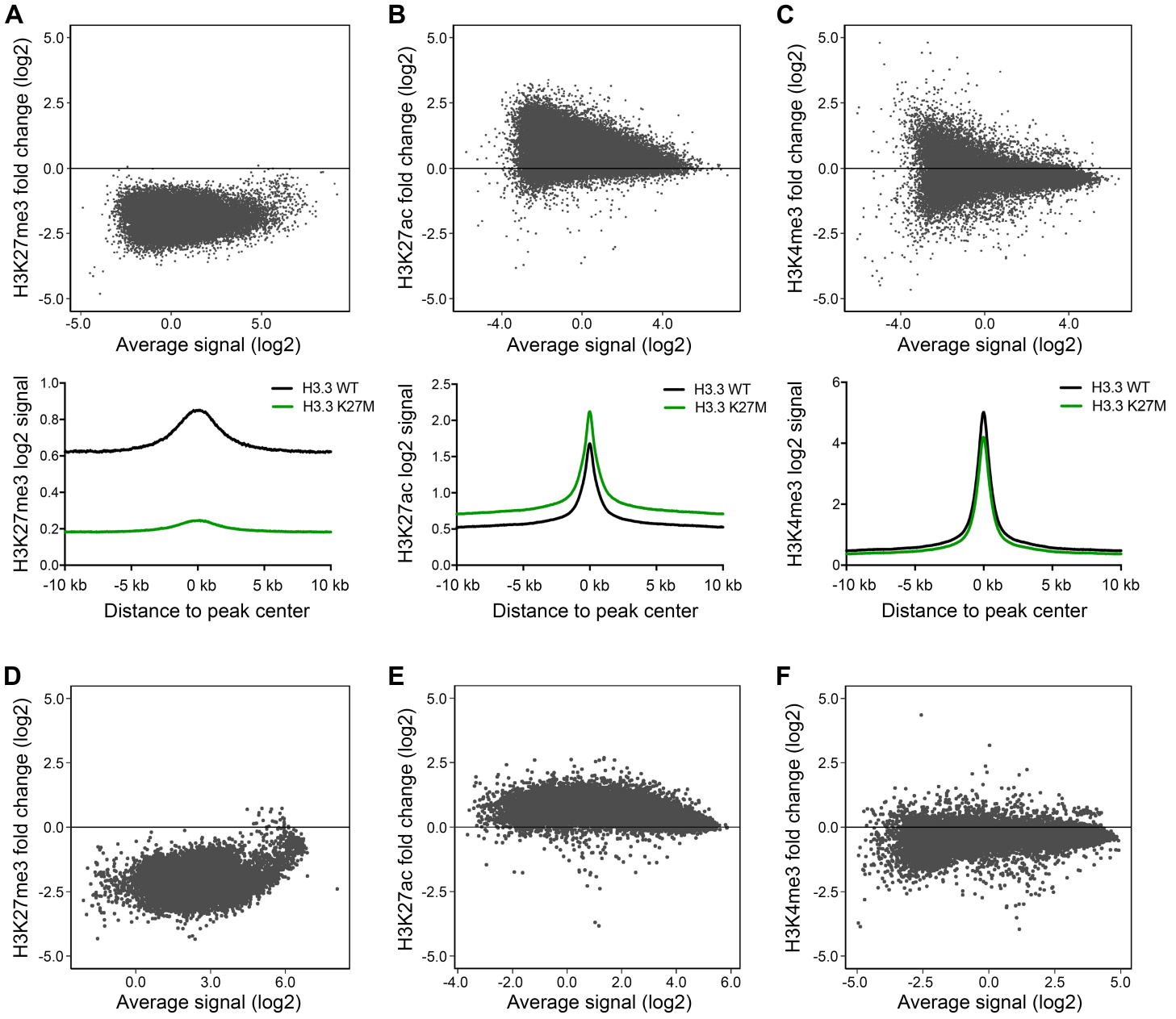

Figure S7 (related to Figure 6). H3.3 K27M Drives Extensive Shifts in H3K27 Methylation and Acetylation Occupancy Across the DIPG Epigenome in H3.3 K27M versus H3.3 WT DIPGs.

(A-C) Peak-based plots depicting average ChIP signal (x axis) relative to log2 fold change (K27M/WT) of ChIP signal (y axis) and demonstrating genome-wide (A) H3K27me3, (B) H3K27ac, and (C) H3K4me3 marks. Corresponding histograms show average signal for H3.3 WT and H3.3 K27M for +/- 10 kb surrounding peak center. (D-F) Promoter-based plots depicting average ChIP signal (x axis) relative to log2 fold change of ChIP signal (y axis) for 2 kb promoter region centered on TSS for (D) H3K27me3, (E) H3K27ac, and (F) H3K4me3 marks. n = 6 (H3.3 K27M) and n = 5 (H3.3 WT) for H3K27me3 and H3K27ac; n = 2 (H3.3 K27M) and n = 3 (H3.3 WT) for H3K4me3.

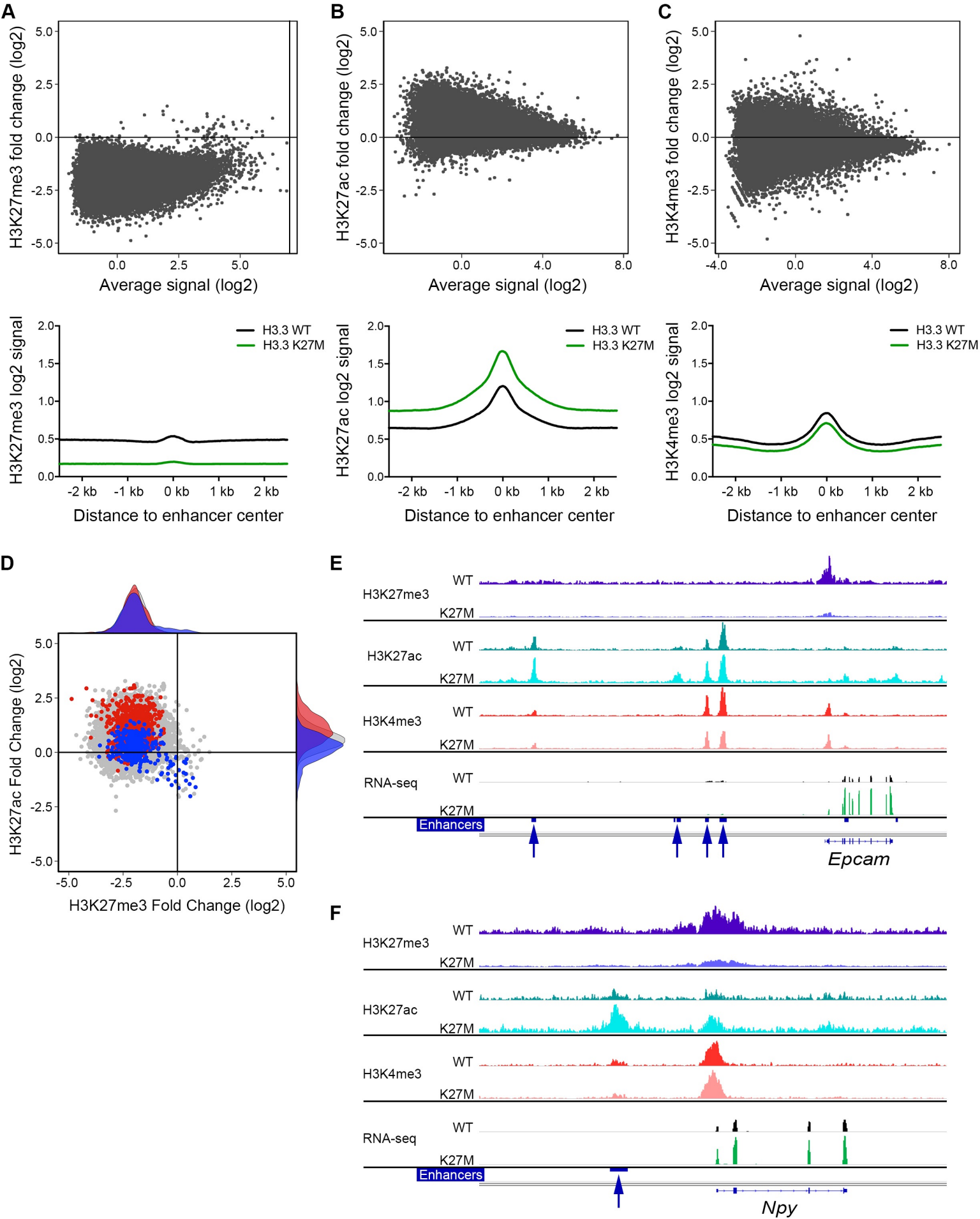
A
H3K27me3 fold change (log2)
Average signal (log2)
B
H3K27ac fold change (log2)
Average signal (log2)
C
H3K4me3 fold change (log2)
Average signal (log2)
H3K27me3 log2 signal
H3.3 WT
H3.3 K27M
Distance to enhancer center
H3K27ac log2 signal
H3.3 WT
H3.3 K27M
Distance to enhancer center
H3K4me3 log2 signal
H3.3 WT
H3.3 K27M
Distance to enhancer center
D
H3K27ac Fold Change (log2)
H3K27me3 Fold Change (log2)
E
H3K27me3
WT
K27M
H3K27ac
WT
K27M
H3K4me3
WT
K27M
RNA-seq
WT
K27M
Enhancers
Epcam
F
H3K27me3
WT
K27M
H3K27ac
WT
K27M
H3K4me3
WT
K27M
RNA-seq
WT
K27M
Enhancers
Npy

Figure S8 (related to Figure 6). Enhancers Reflect Similar Global H3.3 K27M-Dependent Epigenetic Trends as Promoters, but Do Not Appear to be Direct Drivers of H3.3 K27M-Dependent Gene Expression.

(A-C) Active enhancer-based plots depicting average ChIP signal (x axis) relative to log2 fold change (H3.3 K27M/H3.3 WT) of ChIP signal (y axis) for (A) H3K27me3, (B) H3K27ac, and (C) H3K4me3 marks. Corresponding histograms show average signal for H3.3 WT and H3.3 K27M centered on enhancers. (D) Plot of H3.3 K27M/H3.3 WT log2 ratio in mouse DIPGs for active enhancer regions comparing log2 fold change of H3K27ac versus H3K27me3. Colored data points depict genes upregulated (red) and downregulated (blue) in H3.3 K27M tumors with $p < 0.05$ and a log2 fold change greater than 0.75 or less than -0.75, respectively, compared to the enhancer loci bulk (gray). Shaded density histograms illustrate relative overlap of PTM changes at enhancers of up and downregulated genes compared to the gene enhancer of bulk loci that are not significantly changed (gray). Active enhancers were associated with nearest expressed gene. (E,F) Average tracks (identical scale for each genotype pair, promoters on the left) showing H3K27me3, H3K27ac and H3K4me3 enrichment and RNA-seq in H3.3 WT or H3.3 K27M expressing mouse DIPGs for two representative upregulated genes with potentially bivalent promoters, *Epcam* (E) and *Npy* (F). n = 6 (H3.3 K27M) and n = 5 (H3.3 WT) for H3K27me3 and H3K27ac; n = 2 (H3.3 K27M) and n = 3 (H3.3 WT) for H3K4me3; n = 20 (H3.3 K27M) and n = 9 (H3.3 WT) for RNA-seq. Active enhancers are marked with blue bars (blue arrows) below RNA-seq. (A-F) Active enhancers were called based on presence of a H3K27ac peak call in either H3.3 WT or H3.3 K27M samples and being at least 1 kb away from a known promoter.